

# Heavy hadrons production by coalescence plus fragmentation in AA collisions at RHIC and LHC <sup>†</sup>

V. Minissale <sup>1</sup>, S. Plumari <sup>1,2</sup>, G. Coci <sup>1,2</sup>, S.K. Das <sup>2,3</sup> and V. Greco <sup>1,2</sup>

<sup>1</sup> Laboratori Nazionali del Sud, INFN-LNS, Via S. Sofia 62, I-95123 Catania, Italy

<sup>2</sup> Dipartimento di Fisica e Astronomia "Ettore Majorana", Università degli studi di Catania, Via S. Sofia 64, I-95125 Catania, Italy

<sup>3</sup> School of Physical Science, Indian Institute of Technology Goa, Ponda, Goa, India

<sup>†</sup> Presented at Hot Quarks 2018 - Workshop for young scientists on the physics of ultrarelativistic nucleus-nucleus collisions, Texel, The Netherlands, September 7-14 2018

Version November 7, 2018 submitted to Proceedings

**Abstract:** The hadronization process of heavy hadrons with bottom and charm quarks, especially for baryons  $\Lambda_c$ , in a dense QGP medium is largely not understood. We present within a coalescence plus fragmentation model the predictions for  $D^0$  and  $\Lambda_c$  spectra and the related baryon to meson ratios at RHIC and LHC. We will discuss how our model can predict values for  $\Lambda_c/D^0$  of the order of  $O(1)$ , which is much larger than the expectations from fragmentation, and in agreement with early data from STAR collaboration. Furthermore in the same scheme can be predicted a baryon to meson ratio  $\Lambda_c/D^0$  in pp collisions assuming that at the LHC top energies there can be the formation of QGP matter. The results show a considerable volume effects that significantly reduce the ratios, but still predict quite larger values with respect to fragmentation, in agreement with recent data from ALICE in pp collisions.

**Keywords:** Heavy Ion Collision; Hadronization; Heavy quark transport

**PACS:** 25.75.-q; 24.85.+p; 05.20.Dd; 12.38.Mh

## 1. Introduction

Ultra-relativistic heavy ion collision at Large Hadron Collider (LHC) and at Relativistic Heavy-Ion Collider (RHIC) have been designed to reach a new state of matter composed of a strongly interacting plasma of deconfined quark and gluons the so called Quark-Gluon Plasma (QGP). The bulk properties of the matter created are governed by the light quarks and gluons while heavy quarks like charm or bottom quarks are useful probes of the QGP properties [1–12]. In their final state the charm quarks appear as constituent of charmed hadrons mainly  $D$  mesons and  $\Lambda_c, \Sigma_c$  baryons. Recent experimental results from STAR collaboration have shown an enhancement of the baryon/meson ratio in the heavy flavor sector like the one observed for light and strange hadrons compared to the one for p-p collision [13–15]. In particular the experimental data in 10 – 60% central  $Au + Au$  collisions have shown a  $\Lambda_c/D^0 \sim 0.8 \div 1.5$  for  $3 < p_T < 6 \text{ GeV}$  which is a very large enhancement compared to the value predicted by the charm hadron fragmentation ratio for p+p collisions [16]. The idea of the coalescence model comes from the fact that comoving partons in the QGP combine their transverse momentum to produce a final-state meson or baryon with higher transverse momentum [17–20]. Few studies have investigated the modification of the relative abundance of the different heavy hadron species produced. In particular this can manifest in a baryon-to-meson enhancement for charmed hadrons. [21,22]

## 29 2. Coalescence plus Fragmentation Model

The coalescence approach is based on the Wigner formalism, the momentum spectrum of hadrons formed by coalescence of quarks can be written as:

$$\frac{d^2 N_H}{dP_T^2} = g_H \int \prod_{i=1}^n \frac{d^3 p_i}{(2\pi)^3 E_i} p_i \cdot d\sigma_i f_{q_i}(x_i, p_i) f_H(x_1 \dots x_n, p_1 \dots p_n) \delta^{(2)} \left( P_T - \sum_{i=1}^n p_{T,i} \right) \quad (1)$$

30 where  $d\sigma_i$  denotes an element of a space-like hypersurface,  $g_H$  is the statistical factor to form a  
 31 colorless hadron while  $f_{q_i}$  are the quark (anti-quark) phase-space distribution functions for  $i$ -th quark  
 32 (anti-quark).  $f_H(x_1 \dots x_n, p_1 \dots p_n)$  is the Wigner function and describes the spatial and momentum  
 33 distribution of quarks in a hadron and can be related to the hadron wave function. The Wigner  
 34 distribution function used has a Gaussian shape in space and momentum,  $f_M(x_1, x_2; p_1, p_2) =$   
 35  $A_W \exp(-\frac{x_{r1}^2}{\sigma_r^2} - p_{r1}^2 \sigma_r^2)$  where  $x_{r1}$  and  $p_{r1}$  are the 4-vectors for the relative coordinates.  $A_W$  is a  
 36 normalization constant fixed to guarantee that in the limit  $p \rightarrow 0$  we have all the charm hadronizing.  
 37 While  $\sigma_r$  is the covariant width parameter and it can be related to the oscillator frequency  $\omega$  by  
 38  $\sigma = 1/\sqrt{\mu\omega}$  where  $\mu = (m_1 m_2)/(m_1 + m_2)$  is the reduced mass. The width of  $f_M$  can be related to  
 39 the size of the hadron and in particular to the root mean square charge radius of the meson. For  $D^+$   
 40 meson  $\langle r^2 \rangle_{ch} = 0.184 \text{ fm}^2$  corresponding to a  $\sigma_p = \sigma_r^{-1} = 0.283 \text{ GeV}$ ; for  $\Lambda_c^+$  the widths are fixed by  
 41 the mean square charge radius of  $\Lambda_c^+$  which is given by  $\langle r^2 \rangle_{ch} = 0.15 \text{ fm}^2$ .

42 We compute the coalescence probability  $P_{coal}$  for each charm quark then we can assign a probability  
 43 of fragmentation as  $P_{frag}(p_T) = 1 - P_{coal}(p_T)$ . Therefore the hadron momentum spectra from the  
 44 charm spectrum  $dN_{frag}/d^2 p_T dy$  that do not undergo to coalescence is given by the convolution  
 45 with the fragmentation function, for  $D$  and  $\Lambda_c^+$  we employ the Peterson fragmentation function [?] ]

46  $D_{had}(z, Q^2) \propto 1/\left[ z \left[ 1 - \frac{1}{z} - \frac{\epsilon_c}{1-z} \right]^2 \right]$ , where  $\epsilon_c$  is a free parameter to fix the shape of the fragmentation  
 47 function and is determined assuring that the experimental data on  $D$  and  $\Lambda_c$  production in  $p + p$   
 48 collisions are well described by a fragmentation hadronization mechanism. The value it has been fixed  
 49 to  $\epsilon_c = 0.06$  and  $\epsilon_c = 0.12$  as discussed in [5]. The relative ratios between different hadron channels  
 50 are properly calculated and normalized according to the ratio of fragmentation fraction in [16].

### 51 2.1. Fireball parameters and quark distribution

52 We consider the systems created at RHIC in Au+Au collisions at  $\sqrt{s_{NN}} = 200 \text{ GeV}$  and at  
 53 LHC in Pb+Pb collisions at  $\sqrt{s_{NN}} = 2.76 \text{ TeV}$ . Our approach is based on a fireball where the bulk  
 54 of particles is a thermalized system of gluons and  $u, d, s$  quarks and anti-quarks. The fireball is  
 55 considered at  $\tau = 7.8 \text{ fm}/c$ , for LHC, and  $\tau = 4.5 \text{ fm}/c$ , for RHIC, and the system has a temperature  
 56 of  $T_C = 165 \text{ MeV}$ . To take into account for the collective flow, we assume a radial flow profile as  
 57  $\beta_T(r_T) = \beta_{max} \frac{r_T}{R}$ , where  $R$  is the transverse radius of the fireball. For partons at low transverse  
 58 momentum,  $p_T < 2 \text{ GeV}$ , hence we consider a thermal distribution, instead for  $p_T > 2.5 \text{ GeV}$ , we  
 59 consider the minijets that have undergone the jet quenching mechanism. For heavy quarks we use  
 60 the transverse momentum distribution obtained by solving the relativistic Boltzmann equation [5]  
 61 giving a good description of  $R_{AA}$  and  $v_2$  of  $D$  mesons. The heavy quark numbers are estimated to be  
 62  $dN_c/dy \simeq 2$  at RHIC and  $dN_c/dy \simeq 15$  at LHC in agreement with the energy dependence of charm  
 63 production cross section [23]. In the following calculation the charm quark mass used is  $m_c = 1.3 \text{ GeV}$ .

## 64 3. Results

65 The coalescence probability is a decreasing function with  $p_T$ , and at low  $p_T$  having a coalescence  
 66 probability for  $\Lambda_c$  even larger than for  $D^0$  is a quite peculiar feature of the coalescence mechanism  
 67 that we expect to lead to large values of the  $\Lambda_c/D^0$  ratio [22]. In Fig.1(a) are shown the transverse  
 68 momentum spectra at midrapidity for  $Au + Au$  collisions at  $\sqrt{s} = 200 \text{ GeV}$  and for  $(0 - 10\%)$  centrality

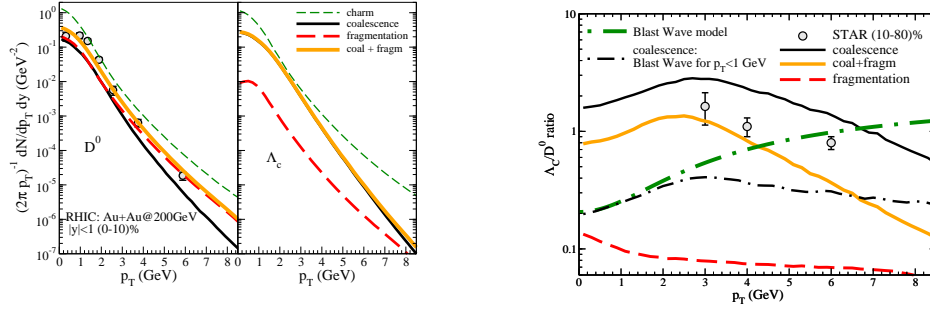


**Figure 1.** (Color online) (a)(left) Transverse momentum spectra at mid-rapidity for Au + Au collisions at  $\sqrt{s} = 200$  GeV and for (0–10%) centrality for  $D^0$  meson (left panel) and for  $\Lambda_c^+$  baryon (right panel). Experimental data taken from [25] (b)(right)  $\Lambda_c^+$  to  $D^0$  ratio as a function of  $p_T$  and at mid-rapidity for Au + Au collisions at  $\sqrt{s} = 200$  GeV and for (10–60%) centrality. Experimental data taken from [15,24].

69 for  $D^0$  meson (left panel) and for  $\Lambda_c^+$  baryon (right panel), we can see that for  $D^0$  the contribution  
 70 of both mechanism is about similar for  $p_T < 3$  GeV and at higher  $p_T$  the fragmentation becomes  
 71 the dominant. For  $\Lambda_c^+$  and  $D^0$  we have included the main hadronic channels that comes from  $D^{*0}$ ,  
 72  $D^{*+}$ ,  $\Sigma_c^*$ (2520) and  $\Sigma_c$ (2455). The coalescence mechanism is the dominant mechanism for the  $\Lambda_c^+$   
 73 production for  $p_T < 7$  GeV and it is mainly related to the fragmentation fraction from the analysis in  
 Ref. [16], where this fraction is about the 6% of the total produced heavy hadrons. In Fig.1 (b) we show

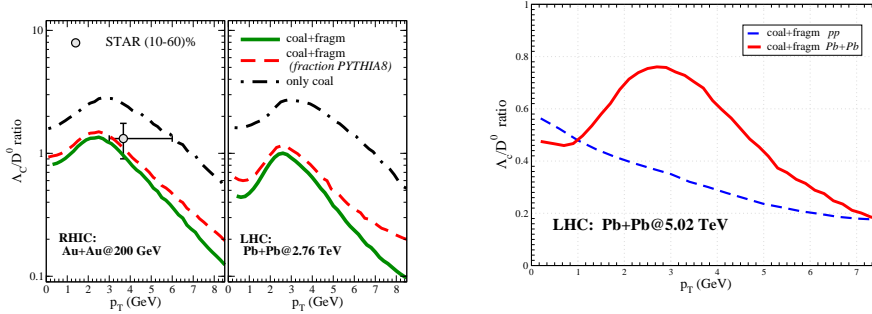


**Figure 2.** (Color online) (a)(left)  $\Lambda_c^+$  to  $D^0$  ratio as a function of  $p_T$  and at mid-rapidity for Au + Au collisions at  $\sqrt{s} = 200$  GeV (left panel) and for Pb + Pb collisions at  $\sqrt{s} = 2.76$  TeV (right panel). (b)(right)  $\Lambda_c^+$  to  $D^0$  ratio as a function of  $p_T$  and at mid-rapidity for Pb + Pb collisions at  $\sqrt{s} = 5.02$  TeV

74 the results for the  $\Lambda_c^+ / D^0$  ratio in comparison with the STAR experimental data shown by circle [15,24].  
 75 Coalescence by itself predicts a rise and fall of the baryon/meson ratio, the inclusion of fragmentation  
 76 reduces the ratio, and we can see a quite good agreement with the experimental data in the peak region  
 77 (orange solid line). In Fig.2 (a) is shown the comparison between RHIC and LHC for the  $\Lambda_c^+ / D^0$  ratio.  
 78 Coalescence predicts a similar ratio for both energies, and the same for fragmentation, because the  
 79 ratio established from the experimental measured fragmentation fraction remains the same changing  
 80 the collision energy. Even if the only coalescence and the only fragmentation ratio remain similar, the  
 81 combined ratio is different because, for each species, the production ratio between coalescence and  
 82 fragmentation is smaller at LHC than at RHIC. Therefore, at LHC the larger contribution in particle  
 83 production from fragmentation [22,26] leads to a final ratio that is smaller than at RHIC. A baryon  
 84 over meson ratio that is so large at low momenta, can lead also to a smaller  $D^0 R_{AA}$  in this region. It is  
 85 consequence of the charm quark number conservation and the dominance of  $D$  mesons in the total  
 86 particle production, in  $pp$  collisions.  
 87

88 In recent years there has been a broadly discussed idea about the possible formation of QGP  
 89 also in systems smaller than the one formed in heavy ion collision. We have applied our model in

90 the case of  $pp$  collisions, assuming that a medium is formed also in this small system like the one  
 91 simulated in hydrodynamics calculations [27]. In Fig.2(b) is shown with the blue dashed line the  
 92  $\Lambda_c^+ / D^0$  ratio obtained for this kind of system. Our calculations predict the disappearance of the peak,  
 93 but an enhancement at low momenta that is significantly different from the ratio obtained with the  
 94 only fragmentation. Moreover, the presence of a coalescence mechanism can have a deep impact on the  
 95  $pp$  baseline used to evaluate the  $R_{AA}$ , in particular in the case of  $\Lambda_c$ , where the presence of coalescence  
 96 implies a different behavior especially at low momenta. This point is still completely open, because of  
 97 the not yet available experimental data.

## 98 References

- 99 1. M. He, R.J. Fries, R. Rapp, Phys. Rev. Lett. **110**(11), 112301 (2013).
- 100 2. J. Uphoff, O. Fochler, Z. Xu, C. Greiner, Phys. Lett. **B717**, 430 (2012).
- 101 3. S. Cao, G.Y. Qin, S.A. Bass, Phys. Rev. **C92**(2), 024907 (2015).
- 102 4. M. Nahrgang, J. Aichelin, S. Bass, P.B. Gossiaux, K. Werner, Phys. Rev. **C91**(1), 014904 (2015).
- 103 5. F. Scardina, S.K. Das, V. Minissale, S. Plumari, V. Greco, Phys. Rev. **C96**(4), 044905 (2017).
- 104 6. S.K. Das, M. Ruggieri, F. Scardina, S. Plumari, V. Greco, J. Phys. **G44**(9), 095102 (2017).
- 105 7. S.K. Das, S. Plumari, S. Chatterjee, J. Alam, F. Scardina, V. Greco, Phys. Lett. **B768**, 260 (2017).
- 106 8. S.K. Das, F. Scardina, S. Plumari, V. Greco, Phys. Lett. **B747**, 260 (2015).
- 107 9. S.K. Das, F. Scardina, S. Plumari, V. Greco, Phys. Rev. **C90**, 044901 (2014).
- 108 10. S.K. Das, J.M. Torres-Rincon, L. Tolos, V. Minissale, F. Scardina, V. Greco, Phys. Rev. **D94**(11), 114039 (2016).
- 109 11. S. Cao, T. Luo, G.Y. Qin, X.N. Wang, Phys. Rev. **C94**(1), 014909 (2016).
- 110 12. R. Rapp *et al.*, Nucl. Phys. A **979**, 21 (2018) doi:10.1016/j.nuclphysa.2018.09.002 [arXiv:1803.03824 [nucl-th]].
- 111 13. X. Dong, Nucl. Phys. **A967**, 192 (2017).
- 112 14. G. Xie, Nucl. Phys. **A967**, 928 (2017).
- 113 15. L. Zhou, Nucl. Phys. **A967**, 620 (2017).
- 114 16. M. Lisovyi, A. Verbytskyi, O. Zenaiev, Eur. Phys. J. **C76**(7), 397 (2016).
- 115 17. R.J. Fries, B. Muller, C. Nonaka, S.A. Bass, Phys. Rev. Lett. **90**, 202303 (2003).
- 116 18. V. Greco, C. Ko, P. Levai, Phys.Rev. **C68**, 034904 (2003).
- 117 19. V. Minissale, F. Scardina, V. Greco, Phys. Rev. **C92**(5), 054904 (2015).
- 118 20. D. Molnar, S.A. Voloshin, Phys. Rev. Lett. **91**, 092301 (2003).
- 119 21. Y. Oh, C.M. Ko, S.H. Lee, S. Yasui, Phys. Rev. **C79**, 044905 (2009).
- 120 22. S. Plumari, V. Minissale, S. K. Das, G. Coci and V. Greco, Eur. Phys. J. C **78**, no. 4, 348 (2018)
- 121 23. J. Adam, et al., Phys. Rev. **C94**(5), 054908 (2016).
- 122 24. X. Dong, arXiv:1810.00996 [nucl-ex].
- 123 25. L. Adamczyk, et al., Phys. Rev. Lett. **113**(14), 142301 (2014).
- 124 26. B. Abelev, et al., JHEP **09**, 112 (2012).
- 125 27. R. D. Weller and P. Romatschke, Phys. Lett. B **774**, 351 (2017)

126 © 2018 by the authors. Submitted to *Proceedings* for possible open access publication  
 127 under the terms and conditions of the Creative Commons Attribution (CC BY) license  
 128 (<http://creativecommons.org/licenses/by/4.0/>).